Journal of the Arkansas Academy of Science

Volume 76 Article 5

2022

Seasonal Testicular Histology and Acystic Lobular Spermatogenesis in the Western Lesser Siren, Siren intermedia nettingi (Caudata: Sirenidae)

Stanley E. Trauth
Arkansas State University (Emeritus), trauthse@outlook.com

Seasonal Testicular Histology and Acystic Lobular Spermatogenesis in the Western Lesser Siren, Siren intermedia nettingi (Caudata: Sirenidae)

Cover Page Footnote

Collection of western lesser sirens was authorized by the Arkansas Game and Fish Commission under annual scientific collecting permits Also, I am grateful to the many graduate students at Arkansas State University for their field assistance.

Seasonal Testicular Histology and Acystic Lobular Spermatogenesis in the Western Lesser Siren, *Siren intermedia nettingi* (Caudata: Sirenidae)

S. E. Trauth

Department of Biological Sciences, Arkansas State University (Emeritus), State University, AR 72467-0599

Correspondence: strauth@astate.edu

Running Title: Seasonal Testicular Histology in the Western Lesser Siren

Abstract

I investigated the seasonal testicular histology and acystic lobular spermatogenesis in the Western Lesser Siren, *Siren intermedia nettingi*, from periodic sampling of this salamander over a span of 21 yr (1994-2015) in northeastern Arkansas. My results include the following general findings: 1) the largest testicular lobules occurred primarily in January-February during spermiogenesis and maturation of spermatozoa; 2) lobular regression and spermatogenic cell recrudescence were underway by late March; 3) proliferation of secondary spermatogonia in lobules was prominent in May; 4) transformation of secondary spermatogonia into primary spermatocytes occurred by mid-July, and these cells became larger in diameter through increased nuclear size and by being heavy laden with lipid droplets; 5) lobular diameters gradually increased through the expansion of lobular luminal open space in July-August, and 6) lobular size continued to increase during October-December with lumina containing numerous secondary spermatocytes. Specifically, my primary objective in this study is to present histologically, for the first time, the annual testicular cycle in this species along with an explanation of the unique cellular complexities of acystic lobular spermatogenesis, a process which this sirenid species shares with another genus (*Pseudobranchus*) within the salamander family Sirenidae. No other vertebrates of any kind possess this type of spermatogenesis.

Introduction

Sirenids are eel-like, aquatic perennibranchiate salamanders (family Sirenidae) that possess an array of distinctive anatomical, morphological, behavioral, molecular, and reproductive features that make their phylogenetic placement within the order Caudata questionable by many scholars (e.g., Cope 1889; Goin and Goin 1962; Goin *et al*. 1978; Frost *et al*. 2006; Zhang and Wake 2009; Pyron and Wiens 2011).

Among the more notable characters of the two genera (*Siren* and *Pseudobranchus*) of this family are the lack of a pelvic girdle and hindlimbs (Martof 1973, 1974 and others). The possession of biflagellated spermatozoa (Austin and Baker 1964; Scheltinga and Jamieson 2003), the unique reproductive process of "non-cystic" lobular spermatogenesis (Trauth *et al.* 2017), and the lack of cloacal glands (Sever 1991) to produce spermatophores in males and sperm storage glands (spermathecae) in females are additional features that distinguish these caudates from all other salamanders. Furthermore, during the process of spermatogenesis, testicular lobules do not develop clonal spermatic cysts as seen in all other anamniotes (fishes and amphibians; see Yoshida 2016).

There is a dearth of published accounts on the male reproductive anatomy in the Western Lesser Siren (*Siren intermedia nettingi*). In his comprehensive summary of the literature on this species, Martof (1973) noted that males reach sexual maturity at 180 mm snout-vent length but mentioned nothing about male reproduction or the testicular cycle. Willett (1965) illustrated the gross anatomy of the urogenital system in this species and in other sirenids, and Sever *et al.* (1996) briefly described the male reproductive cycle in *S. i. intermedia* from a population in South Carolina. However, the latter authors provided no histological images on seasonal variation in the testes.

The seasonal activity pattern in *S. i. nettingi* in their preferred habitats (sloughs and vegetated aquatic ditches) in northeastern Arkansas (Trauth *et. al.* 2004) is mostly unpredictable and largely dependent upon local weather and habitat conditions. The species often remains inactive during summer months and is nearly impossible to collect during drought periods (Sawyer and Trauth 2012).

As part of a long-term investigation on the male reproductive anatomy of *S. i. nettingi*, I present here the first histological analysis of the seasonal testicular cycle and a description of acystic lobular spermatogenesis in this species. In forthcoming contributions on spermiogenesis and spermatozoal morphology in this salamander, I will provide detailed information pertaining to the process of spermiation via scanning electron microscopy (SEM), report on the structure of the biflagellated spermatozoon using SEM, and characterize spermatological structures using transmission electron microscopy.

Materials and Methods

I histologically examined the testes of a selected group of 22 adult *S. i. nettingi* collected periodically from northeastern Arkansas from 1994-2015 using seines, dip nets, and minnow traps. I euthanized the salamanders by submersion in a dilute chloretone solution in accordance with IACUC protocol regulations and guidelines at Arkansas State University. In most cases, I excised cross-sectional segments of the testes and placed them into either vials of 10% neutral buffered formalin, NBF (see comments below for procedures for paraffin sectioning–LM-Paraffin) or into vials of 2% glutaraldehyde (GTA) solution buffered with 0.1 M sodium cacodylate at a pH of 7.2 (see below for procedures for semi-thin plastic sectioning–LM-Plastic) for 2 h. I used 1% osmium tetroxide, buffered as above for 2 h, for postfixation of GTA-fixed tissues to enhance the preservation and staining of cytoplasmic lipids.

Following necropsy and tissue extraction, most salamanders were measured (snout-vent length [SVL] to the nearest in mm), fixed in 10% NBF, and later preserved in 70% ethanol. Each salamander was assigned an Arkansas State University Museum of Zoology (ASUMZ) number and documented (ASUMZ no., SVL [if recorded], and date of collection; see Specimens Examined): Salamanders are deposited in the herpetological collection in the Arkansas Center for Biodiversity Collections at Arkansas State University.

The testes were prepared for LM-Paraffin and LM-Plastic in the former Electron Microscope Facility at Arkansas State University. These histological procedures have been recently described in detail elsewhere (Trauth 2020, 2021). For LM-Paraffin (as viewed in Fig. 1), I followed the paraffin embedding techniques outlined in Presnell and Schreibman (1997), and I used Pollak trichrome stain to stain this section of an entire testis. For LM-Plastic for epoxy-embedded testes, I arranged the transversely cut segments into several smaller tissue blocks. For semi-thin sectioning (approximately 1 µm in thickness) of these blocks, I followed prep techniques outlined in Dawes (1988). I then used glass knives on an LKB Ultrotome (Type 8800) and applied Ladd® multiple stain (LMS) for contrast enhancement of tissues.

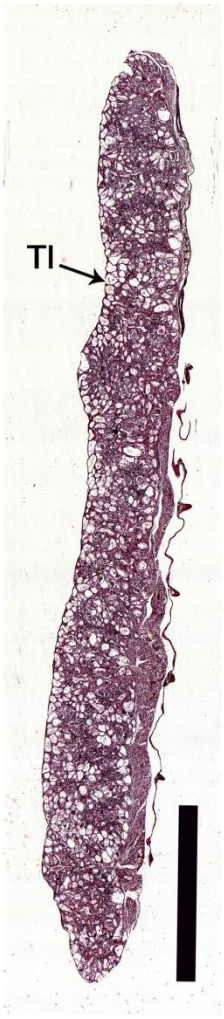

Figure 1. Light micrograph (LM-Paraffin) of a longitudinal section through the left testis of *Siren intermedia nettingi* from a February specimen (ASUMZ 22274). Tl, testicular lobule. Scale bar = 5 mm.

For photomicroscopy, I used either a Nikon Eclipse E600 compound light microscope attached to a Nikon DXM 1200 digital camera or a Leica MC 120 HD camera atop a Leica DM 2000 LED compound light microscope. Also, I employed a PrimeHisto XE slide scanner (Carolina Biological Supply Co., Burlington, NC) to capture the testicular image in Figure 1. Numerical computations followed standard statistical methods; means were followed by ± one standard deviation. Most of the terminology regarding

https://scholarworks.uark.edu/jaas/vol76/iss1/5
DOI: 10.54119/jaas.2022.7604

testicular anatomy followed Trauth *et al.* (2017). Microscope slides are currently catalogued and housed in the Trauth Histo-herpetology Laboratory in Morrilton, Arkansas.

The sequential cellular stages of acystic lobular spermatogenesis in *S. i. nettingi* do not conform to or align with any typical developmental processes leading to the release of sperm aggregates or bundles into lobular lumina as observed in cystic lobular spermatogenesis found in all salamanders outside of the family Sirenidae (see Uribe 2003; Ogielska and Bartmańska 2009; Uribe and Mejía-Roa 2014) and in all fishes (Uribe *et al*. 2014). The morphology of maturing, spermiogenic cells can only be characterized as extraordinary when compared to their anatomical counterparts found in amphibians and fishes and incomparable to stages found in any higher vertebrate species. Although quite remarkable in cell structure and composition, I, nevertheless, employed the names of typical cell types defined within the three principal phases of vertebrate spermatogenesis (e.g., spermatocytogenesis, meiosis, and spermiation) as outlined by Ross *et al.* (1989) and detailed for salamanders by Uribe and Mejía-Roa (2014).

In presenting the following histological images of the testicular lobules and spermatogenic stages (Figs. 2 – 7), I sought to explain the testicular cycle in terms of monthly sequential events associated with spermatogenic cell types contained within lobules specifically to document an entire seasonal cycle. This mirrored the approach by Sever *et al.* (1996). However, because different spermatogenic stages and cell types of acystic lobular spermatogenesis may occur not only within the same testis but also in testes at multiple time periods, there will be some monthly discordance in presenting these progressive changes as recorded chronologically in my histological figures.

Results and Discussion

In their paper on reproduction in *S. i. intermedia* from South Carolina, Sever *et al.* (1996) described the male cycle in a brief manner, and I have reproduced below their comments in its entirety:

"Testicular lobules from specimens collected in January were filled largely with spermatids indicating the imminent onset of spermiation. No males were present in the February sample, but mature spermatozoa were abundant in the testes and vasa efferentia males collected in March, and some spermatozoa were present in a specimen examined on 4 May. In late June testicular lobules were filled with primary spermatogonia. In a male from the September collection, proliferation of the spermatogonia was evident, and lumina of the testicular lobules were lined with secondary spermatogonia. Thus maturation and transfer of sperm into the reproductive occurred between January and March."

In general, my results provide histological support for these descriptive findings. Their primary focus, however, was to examine female oviductal anatomy, and they neglected to document how many of the 34 males they collected were used in their descriptive analysis. Unfortunately, they did not provide critical cell dimensions or any detailed cytological information on the spermatogenic cells of this eastern subspecies. Also, it is paramount to point out that their descriptive interpretations followed closely a classic work on cystic lobular spermatogenesis available at that time for amphibians (i.e., Uribe *et al.* 1994). As in all sirenids presently examined (i.e., *Siren lacertina* [Hanlin and Mount 1978] and *Pseudobranchus axanthus* [Trauth *et al.* 2017]), the testes of *S. i. nettingi* are comprised of numerous lobules (Fig. 1) which undergo an annual and mostly synchronous cycling in size and epithelial cell complexity among most adult males.

January-February. – The histological changes in the testicular lobules of *S. i. nettingi* observed in the present study mostly adhere to the descriptions of the spermatogenic cycle as described by Sever *et al.* (1996). In northeastern Arkansas, testes of most winter-collected males exhibited expanded testicular lobules of varying lengths and widths (Figs. 1; 2A – D; 5A). For example, lobular diameters ranged from 270 – 530 µm ($\overline{x}$ = 399.39 ±61.01; n = 49). The interior walls of the lobules were lined with a single, mostly non-contiguous layer of spermatogenic cells interspersed with Sertoli cells (Figs. 2A, B; 3A). Scattered about within lumina were an assortment of spermiogenic cells including secondary spermatocytes, transforming spermatids (Fig. 3A), mature spermatozoa (Fig. 3C), and some cellular debris (Fig. 3B). Diameters of cell bodies of secondary spermatocytes within lobular lumina varied from 28 – 42 µm ($\overline{x}$ = 34.22 ±3.50; n = 58). The nuclear diameters of these soon-to-transform cells ranged from 19 – 25 µm ($\overline{x}$ = 21.78 ±1.76; n = 23) as seen in Figure 3 (A – D).

The distinctive retention of cytoplasmic lipid droplets and the formation of cellular fibers (Fig. 3D, F) characterize early transforming spermatids during spermiogenesis. The lipid reserves presumably play a vital role as an energy resource in the formation of the cellular fibers and their transformation into the 2 undulating membranes and 2 axonemal fibers that are present in the mature biflagellated spermatozoon

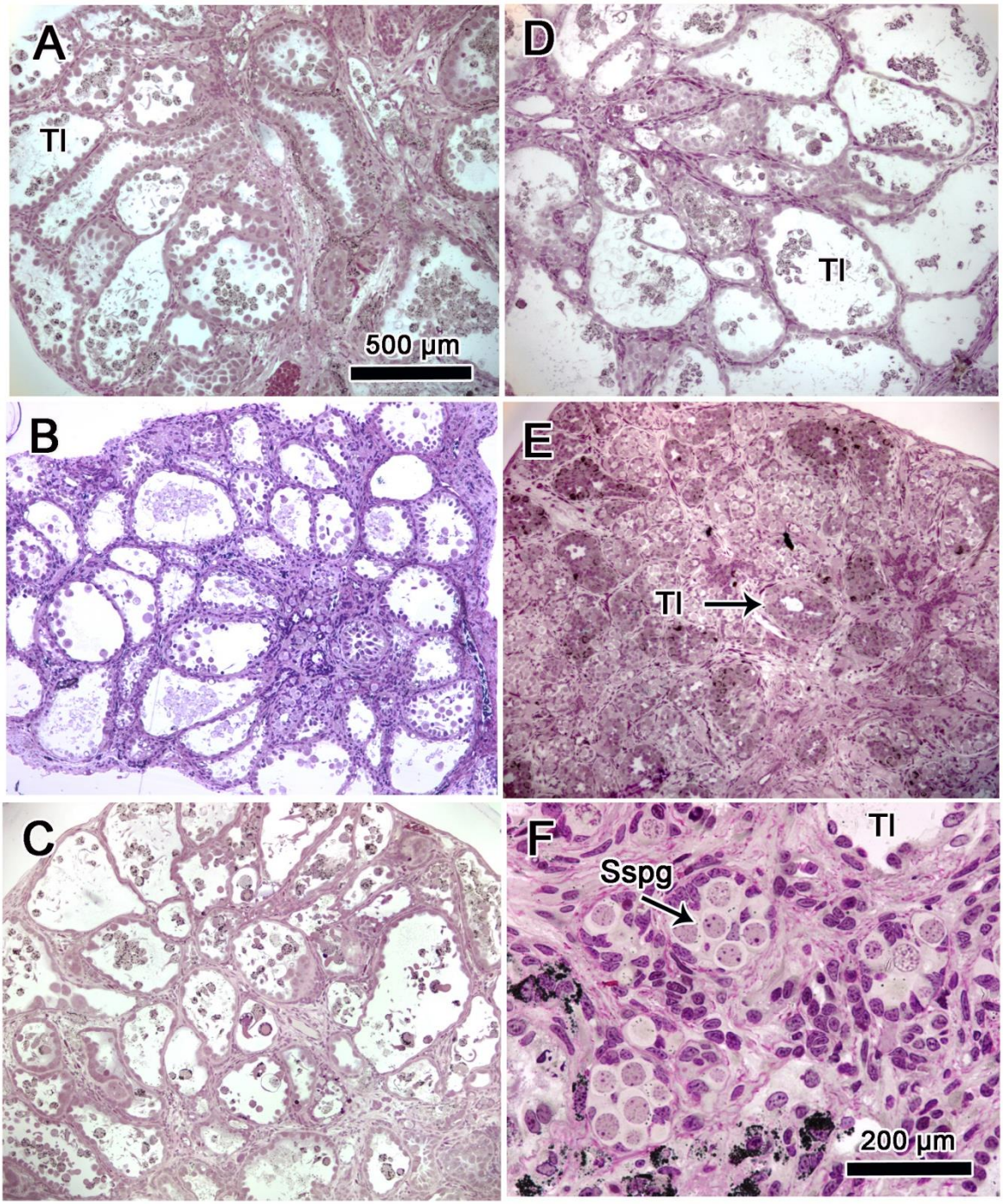

Figure 2. Light micrographs (LM-Plastic) showing transverse sections of testicular lobules of *Siren intermedia nettingi* from January (A-ASUMZ 32416 and B-ASUMZ 30337), February (C-ASUMZ 19342 and D-ASUMZ 31985), and March (E-ASUMZ 32588 and F-ASUMZ 30416). See text for further explanation of images. Sspg, secondary spermatogonium within spermatogonial-Sertoli cell cluster. Abbreviation (Tl) is the same as in Figure 1. Scale bar in A is the same for B – E.

(Austin and Baker 1964; Scheltinga and Jamieson 2003). At least 8 fibers are revealed by examination using transmission electron microscopy (unpubl.). Formation of these fibers is concurrent with spermatid cytoplasmic extrusion and cell elongation (Fig. 3E). The release of individual spermiogenic cells into lobular lumina from their attachments to Sertoli cells on the epithelial lining must occur before completion of the spermatid phase (Fig. 3). This represents a hallmark feature of acystic (a.k.a. "non-cystic" as used by Trauth *et al.* 2017) lobular spermiogenesis in sirenids, as first observed in *P. axanthus* (Trauth *et al.*

https://scholarworks.uark.edu/jaas/vol76/iss1/5
DOI: 10.54119/jaas.2022.7604

2017). Moreover, the peculiar structural nature of the transforming spermatids (Fig. 3D – F) is beyond current descriptive terminology for vertebrate spermatids. The January-February specimens are at the height of reproductive activity, and testes are also nearing the end point of the spermiogenic phase of the spermatogenic cycle. (This terminal phase of spermiogenesis will be more thoroughly addressed in future studies.) Most males examined during this time frame possessed testes undergoing spermiogenesis, although a deviation from this time period (possibly indicative of an extension of the mating season in 2014) did occur in one May salamander (Figs. 3B; 5A).

March. – The testes of March specimens exhibited a rapid transition into the regression and subsequent recrudescence phases of acystic lobular spermatogenesis, which coincides with the waning of the mating season. Testicular size declined sharply as testicular lobules diminished in diameter (range, 180 – 210 µm; $\overline{x}$ = 196.37 ±12.27; n = 11; see Fig. 2E, F) and were devoid of spermatozoa. Aggregates of spent lobules (e.g., see arrows in Fig. 5A) can be seen residing mostly within the interior of regressing testes. Testicular recrudescence is initiated by the process of spermatocytogenesis. Primary spermatogonia are easily recognizable embedded in interior connective tissue outside of regressed lobules (Fig. 2F) and in testes examined from other months during this study (e.g., Fig. 4A). Dimensions of these large stem cells and their nuclei (cell diameters, 30.0 – 62.5 µm; $\overline{x}$ = 42.92 ±7.93; n = 14; nuclear diameters, 22.5 – 30.00 µm; $\overline{x}$ = 24.64 ±2.57; n = 14) are greater than secondary spermatogonia (cell diameters, 21.0 – 33.0 µm; $\overline{x}$ = 27.94 ±3.36; n = 24; nuclear diameters, 13.0 – 21.5 µm; $\overline{x}$ = 19.98 ±2.46; n = 24). A primary spermatogonium is also discernible by the possession of a distinct nuclear envelope (arrows in Fig. 4A) compared to that of a secondary spermatogonium (Fig. 4B – E). In addition, the nucleoplasm of the former is more translucent and exhibits irregular patches of heterochromatin attached to the nuclear envelope compared to the latter (Fig. 4B – F) that possesses more concentric masses of heterochromatin scattered about within a denser, opaque nucleoplasm. Surrounding these dividing germ cells are Sertoli cells, which appear to outnumber the germ cells within a developing lobule. Sertoli cells will remain conspicuous companions of mitotic and meiotic cells throughout the spermatocytogenic and meiotic phases of the spermatogenic cycle.

Oddly, the presence (earliest appearance) of primary spermatocytes was observed in a March specimen (Fig. 7C); however, these cells prevail along the lobular epithelium primarily in July males. In addition, as these spermatogenic cells develop from secondary spermatogonia and increase in size, numerous distinctive cytoplasmic inclusionary bodies (lipid droplets) begin to appear (Figs. 4D; 7A, B). It is assumed that these cells must attain a full complement of lipid droplets prior to the initiation of the meiotic phase (see July-August).

Sever *et al.* (1996) had no male specimens from February, but found mature spermatozoa in males collected in March. In the present study, no specimens were collected in April. However, egg clusters containing well-developed embryos have been observed in early April in northeastern Arkansas (Noble and Marshall 1932), thus indicating that mating probably occurs in March.

May-June. – Testicular recrudescence continues as viewed in a late May specimen (Fig. 5B). Diameters of most testicular lobules have gradually expanded (range, 170 – 310 µm; $\overline{x}$ = 226.00 ±52.80; n = 10) due to the proliferation of secondary spermatogonia (cell diameters, 27.5 – 40.0 µm; $\overline{x}$ = 31.54 ±3.32; n = 26; nuclear diameters, 17.5 – 27.5 µm; $\overline{x}$ = 21.92 ±2.48; n = 26), which are accompanied by numerous nurturing Sertoli cells (Figs. 4D; 5B). As stated earlier, one early May specimen (Fig. 5A) exhibited some expanded lobules characteristic of the January-February time frame and, at the same time, this individual contained scattered groups of totally regressed lobules, indicative of testicular regression (arrows in Fig. 5A). Moreover, the interior linings of these expanded lobules in this male exhibited a non-functional epithelium (see arrow in Fig. 3B) characterized by the lack of spermatogenic cells and Sertoli cells. The lobular lumina also contained mostly cellular debris and residual spermatids.

Testicular lobules in a June male (Fig. 5C) show a similar size (range, 175 – 240 µm; $\overline{x}$ = 224.50 ±21.40; n = 10) to the one in May (i.e., Fig. 5B). In addition, lumina are absent or mostly hidden by the multitude of proliferating secondary spermatogonia. Most interior walls of lobules are now lined with what appears to be a bilayer of secondary spermatogonia and an apical (more interior) scattering of Sertoli cells. The progressive process of lipid deposition into primary spermatocytes continues throughout the spring months and into the fall months at an accelerated rate as more of the cells increase in number and size.

July-August. – By mid-July (Fig. 5D), testicular lobules still resemble those in June, except that lobular diameters are slightly larger (range, 180 – 280 µm; $\overline{x}$ =

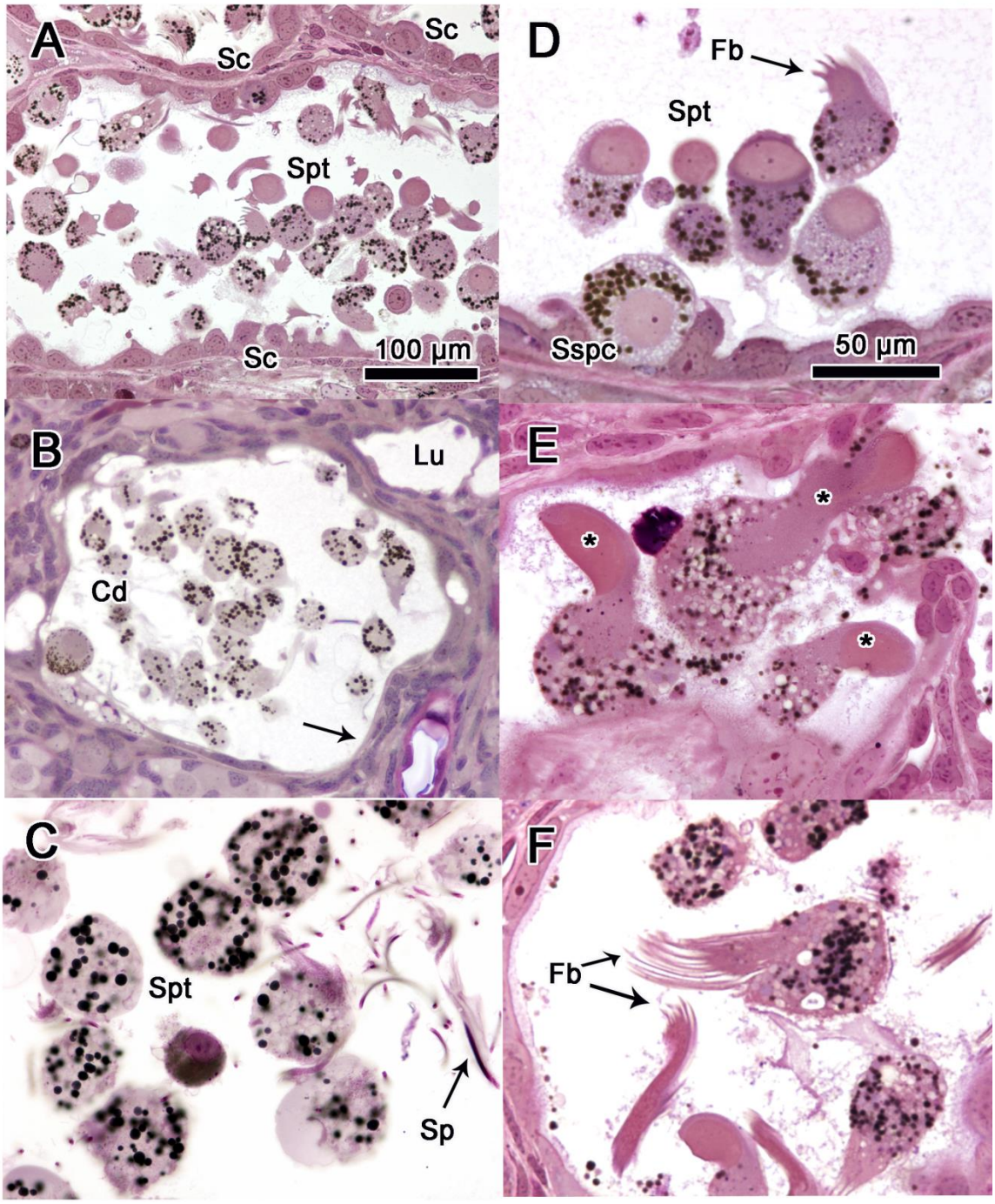

Figure 3. Light micrographs (LM-Plastic) showing transverse sections of testicular lobules of *Siren intermedia nettingi* from January (C-ASUMZ 32416), February (A, D-F-ASUMZ 19342), and May (B-ASUMZ 33189). Cd, cellular debris; Fb, fibers; Lu, lumen; Spt, spermatid; Sp, spermatozoon. Arrow in B points to a cell-depleted lobular lining. Asterisks in E are regions of spermatid elongation. See text for further explanation of images. Scale bar in A is the same for B; in D, the same for C, E, and F).

246.50 ±28.68; n = 10) due to an increase in luminal open area. Secondary spermatogonia had cell diameters (range, 22 – 48 µm; $\bar{x}$ = 29.97 ±5.75; n = 32) and nuclear diameters (range, 13 – 29 µm; $\bar{x}$ = 20.64 ±3.11; n = 33) similar those in the May-June specimens; however, their mitotic divisions (Fig. 4E) have now begun to wane. The appearance of numerous lipid droplets is evident in what are now newly created primary spermatocytes (Figs. 4F; 7A, B), having transformed from secondary spermatogonia. The presence of these cells is an indication that the meiotic phase is now well underway (e.g., Fig. 7A, B).

https://scholarworks.uark.edu/jaas/vol76/iss1/5
DOI: 10.54119/jaas.2022.7604

By mid-August, diameters of testicular lobules (Fig. 5E) have continued to increase in size (range, 230 – 340 µm; $\bar{x}$ = 278.08 ±31.34. n = 26); well-defined lumina are now present. Diameters of primary spermatocytes (range, 50 – 73 µm; $\bar{x}$ = 57.0 ±7.17; n =14) increased in size primarily due to continued lipid deposition (Fig. 5F); also, these cells now possess enlarged nuclear diameters (range, 30 – 37.5 µm; $\bar{x}$ = 32.61 ±2.63; n = 14). As meiosis I progresses, secondary spermatocytes are now becoming more prevalent and possess enlarged cell diameters (range, 35 – 70 µm; $\bar{x}$ = 46.32 ± 8.68; n = 19). Secondary spermatocytes now reside along the basement membrane of the epithelial lining of lobules.

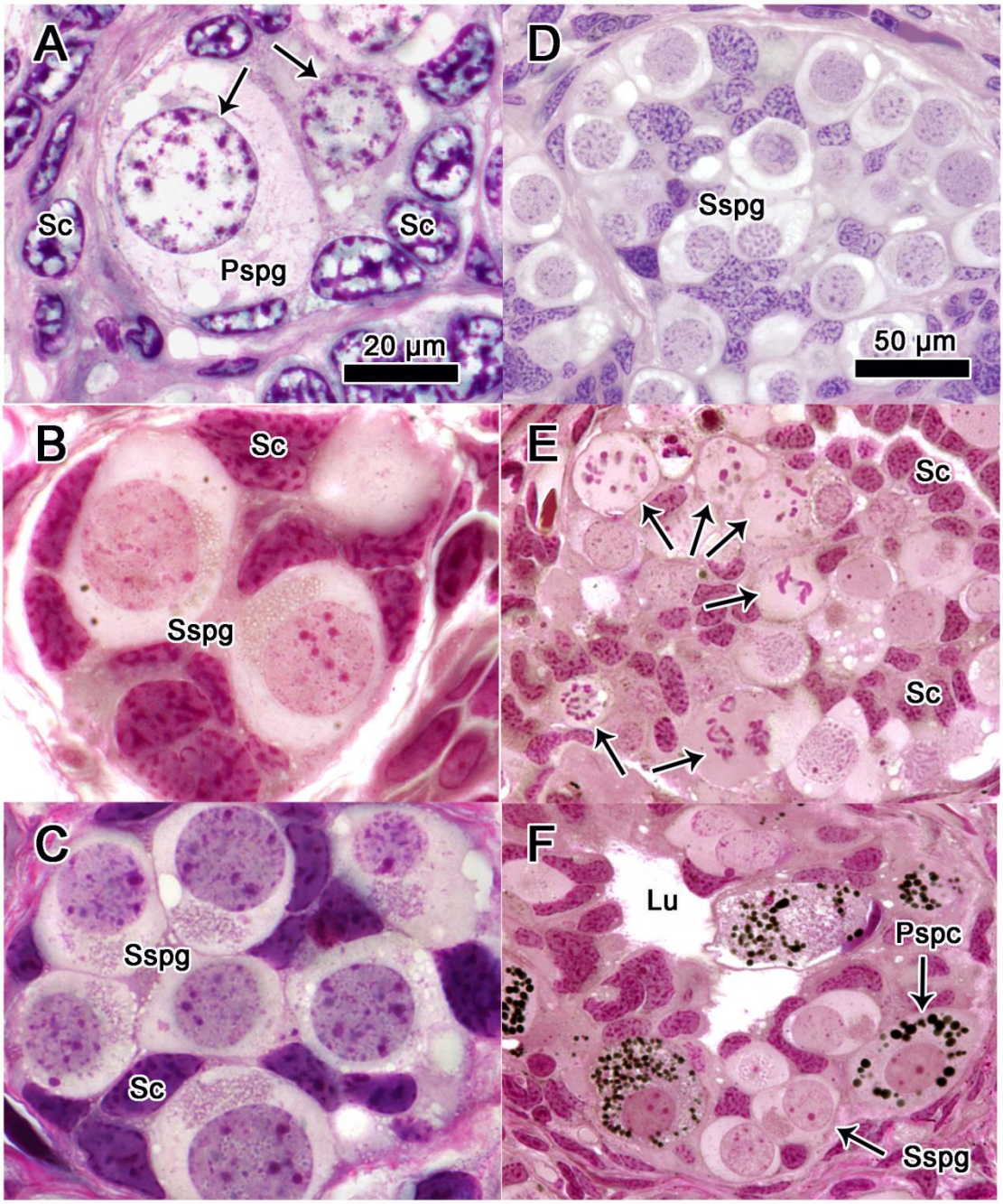

Figure 4. Light micrographs (LM-Plastic) showing transverse sections of testicular lobules of *Siren intermedia nettingi* from August (A-ASUMZ 33370), October (B-ASUMZ 32366), January (C-ASUMZ 30337), May (D-ASUMZ 33201), and July (E, F-ASUMZ 32311). Arrows in A point to nuclear envelope of primary spermatogonium (Pspg). Arrows in E point to mitotic figures of dividing secondary spermatogonia. See text for further explanation of images. Abbreviations are the same as in previous figures. Pspc, primary spermatocyte. Scale bar in A is the same for B and C; in D, the same for E and F.

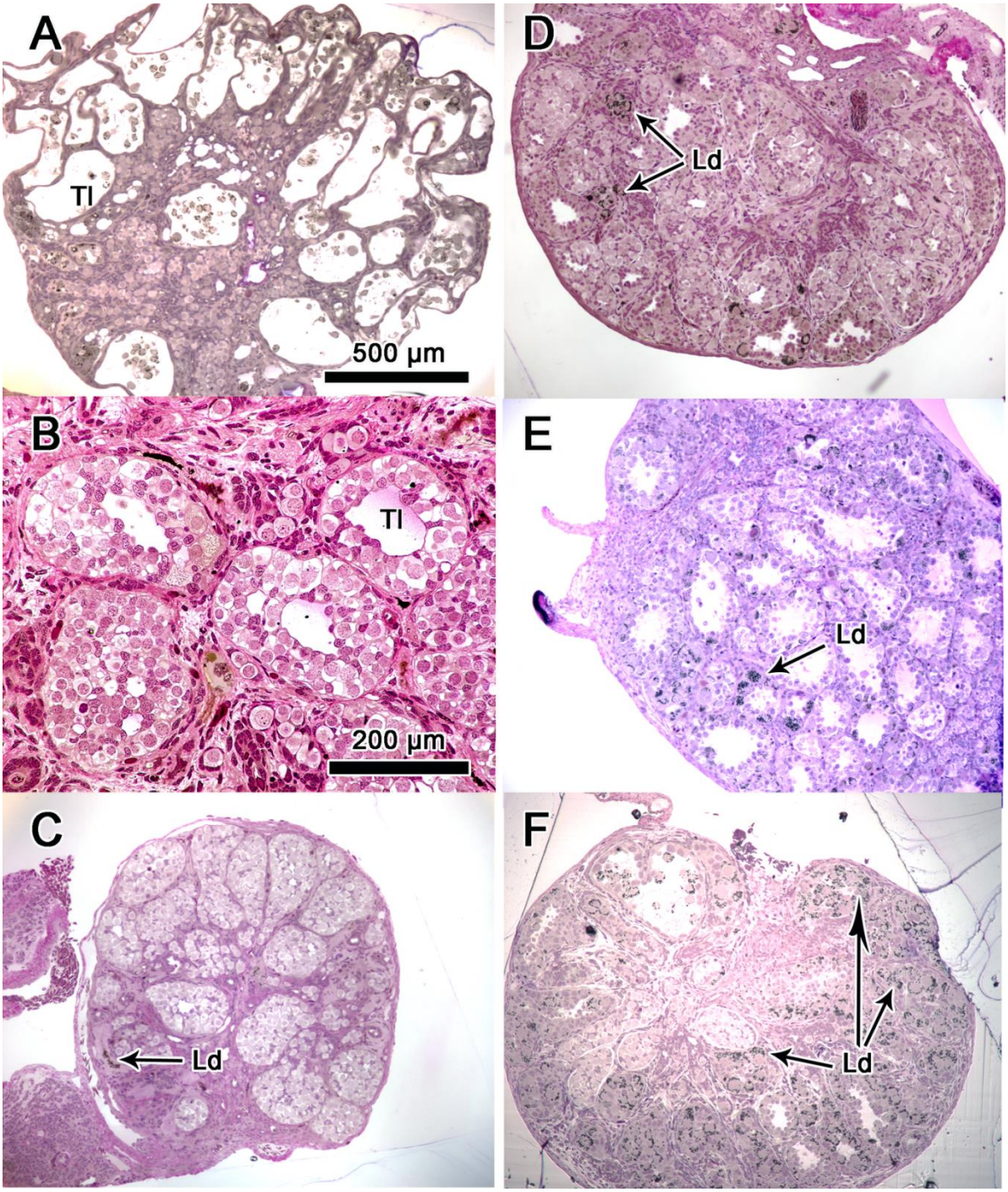

Figure 5. Light micrographs (LM-Plastic) of transverse sections of testicular lobules of *Siren intermedia nettingi* from May (A-ASUMZ 33189 and B-ASUMZ 33201), June (C-ASUMZ 33239), July (D-ASUMZ 32311), August (E-ASUMZ 33370), and October (F-ASUMZ 32366). Abbreviations are the same as in previous figures. See text for explanation of images. Ld, lipid droplets. Scale bar in A is the same for B – F.

October-December. – No sirens were collected during September and November. Testicular lobules from 2 males collected in October (Figs. 5F; 6A, B; 7D – F) exhibited continued expansion of lumina through an increase in their open spaces (range, 165 – 560 µm; $\overline{x}$ = 269.34 ±99.48; n = 29). Primary spermatocytes possessed cell diameters (range, 60 – 77 µm; $\overline{x}$ = 65.16 ±5.28; n = 13) and nuclear diameters (range, 30 – 45 µm; $\overline{x}$ = 34.46 ±5.28; n = 13) similar to the August specimen. Cell size of secondary spermatocytes

https://scholarworks.uark.edu/jaas/vol76/iss1/5
DOI: 10.54119/jaas.2022.7604

(range, 38 – 62 µm; $\bar{x}$ = 48.71 ±8.51; n = 19) and their nuclear diameters (range, 19 – 35 µm; $\bar{x}$ = 24.37 ±3.81; n = 19) were comparable to the August specimens, but slightly larger than those found in the January-February specimens. As lobular diameters expand, secondary spermatocytes begin to move away from the epithelial lining presumably in order to initiate or complete meiosis II (e.g., Figs. 6A; 7F). Moreover, it is plausible to assume that this detachment is a crucial step prior to the onset of the spermatid phase of the spermatogenic cycle. This concept is further supported by the presence of individual secondary spermatocytes within the lumina of January-February specimens (Figs. 2A – D; 3A).

Only one young adult male was collected in December (Fig. 6C). Testicular lobules were in early expansion (range, 132 – 200 µm; $\bar{x}$ = 160.94 ±23.35; n = 8) and occurred mostly along the periphery of the testis Their interior regions (lumina) contained numerous primary spermatogonia, whose cell diameters (range, 35 – 40 µm; $\bar{x}$ = 37.50 ±1.39; n = 14) and nuclear diameters (range, 20 – 27.5 µm; $\bar{x}$ = 24.11 ±2.10; n = 14) were similar to those observed in other males in other months. Primary spermatocytes had acquired lipid droplets (Fig. 6C) and were the most common cell type within lumina. Their cell diameters (range, 47.5 – 62.5 µm; $\bar{x}$ = 51.54 ±4.27; n = 13) and nuclear diameters (range, 25.0 – 32.0 µm; $\bar{x}$ = 27.69 ±2.79; n = 13) were slightly smaller compared to those of the August specimen. Based upon the lack of enlarged lumina and the absence of secondary spermatocytes, it is assumed that this smaller male (SVL = 218 mm) is out of sync with the testicular cycles of larger adult males.

Germ Cell Morphology: Comparisons With Another Caudate. – Acystic lobular spermatogenesis offers ample opportunities for comparing spermatogenic cells of this novel process with those of cystic lobular spermatogenesis of other salamanders. For example, Uribe (2003) stated that primary spermatogonia of *Ambystoma dumerilii* average 40 – 50 µm in diameter and that secondary spermatogonia were similar in size (35 – 45 µm). In the present study, diameters of primary spermatogonia ranged from 30 – 40 µm), whereas secondary spermatogonia ranged from 21 – 48 µm; therefore, these values show a similarity between the two species. Primary spermatocytes of *A. dumerilii* ranged from 35 – 45 µm in diameter and were also similar to those found for secondary spermatogonia, whereas primary

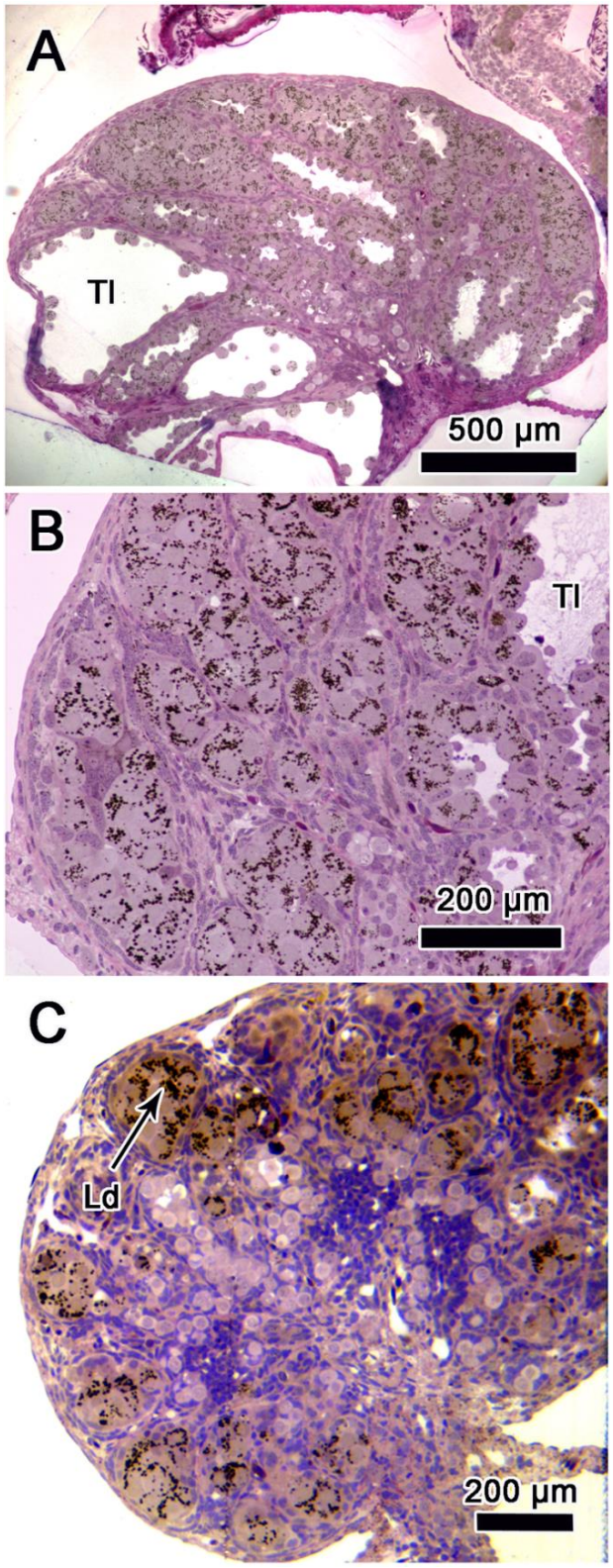

Figure 6. Light micrographs (LM-Plastic) of transverse sections of testicular lobules of *Siren intermedia.nettingi* from October (A, B-ASUMZ 33318) and December (C-ASUMZ 33329). See text for explanation of images. Abbreviations are the same as in previous figures.

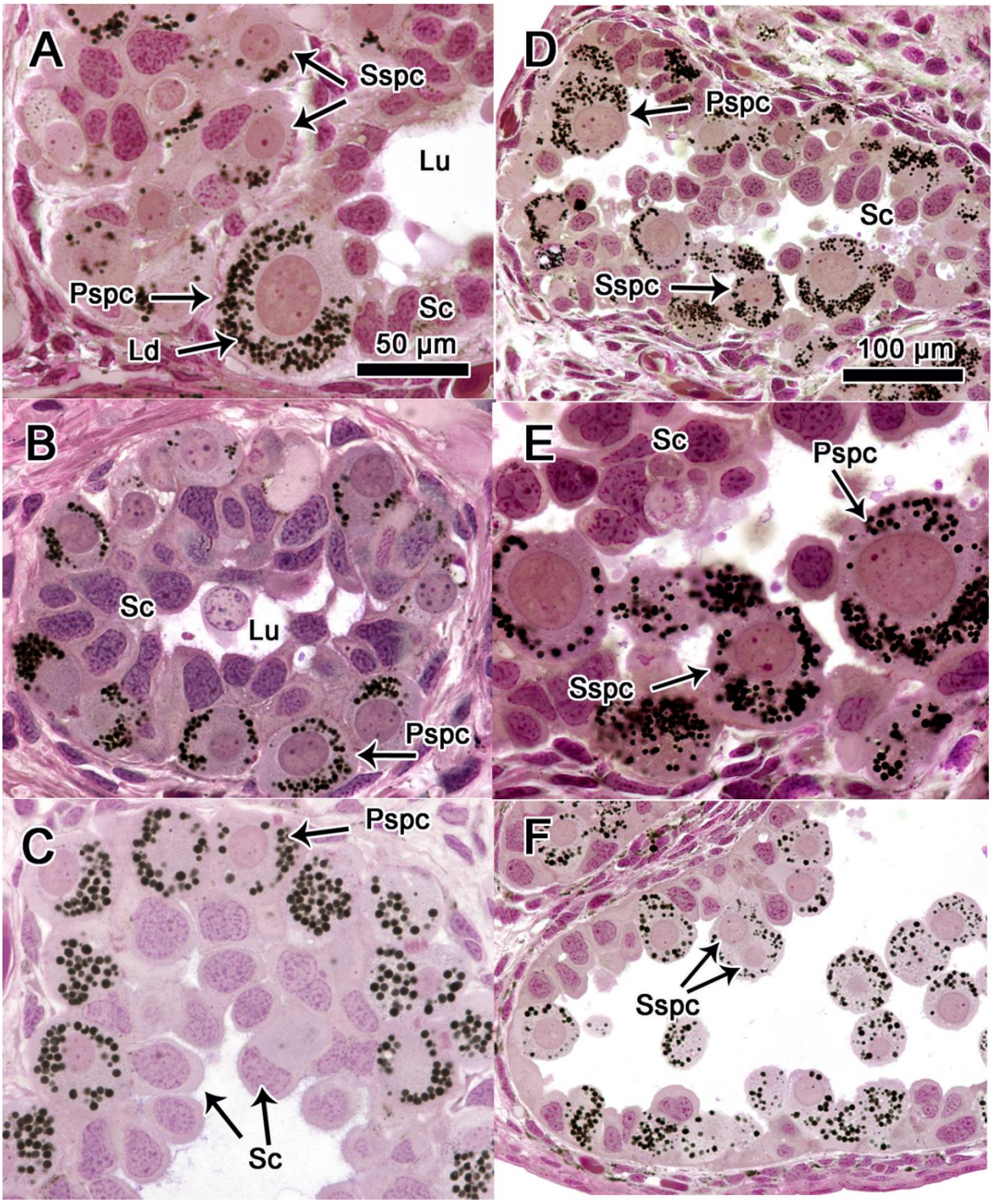

Figure 7. Light micrographs (LM-Plastic) of transverse sections of testicular lobules of *Siren intermedia nettingi* from July (A-ASUMZ 32311 and B-ASUMZ 32309), March (C-ASUMZ 32588), and October (D-F, ASUMZ 32366). Sspc, secondary spermatocyte. See text for explanation of images. Abbreviations are the same as in previous figures. Scale bar in A is the same for B, C, and E; in F the same as in D.

spermatocytes in *S. i. nettingi* ranged from 50 – 77 µm and were much larger than those of *A. dumerilii*. This marked difference in size is attributed to the buildup of lipid droplets found in the cells of *S. i. nettingi.* Secondary spermatocytes of *A. dumerilii* averaged 17 µm, and those of *S. i. nettingi* were much larger (28 –

https://scholarworks.uark.edu/jaas/vol76/iss1/5
DOI: 10.54119/jaas.2022.7604

70 µm) for the same reason as stated above. Finally, spermatids of *A. dumerilii* averaged 15 µm in diameter, whereas the spermatids of *S. i. nettingi* are much larger (22 – 27 µm in diameter, unpubl.). Ogielska and Bartmańska (2009) referred to the diameters of spermatogenic cells from Uribe (2003) in their general summary of caudate spermatogenesis.

Conclusions

The unique process of acystic lobular spermatogenesis represents a stark contrast to the universal process of cystic spermatogenesis found among other anamniotes. Also, my findings lend support to the proposal by Goin and Goin (1962) and Goin *et al.* (1978) that the family Sirenidae should be elevated to the taxonomic ordinal level within the class Amphibia.

Acknowledgments

Collection of western lesser sirens was authorized by the Arkansas Game and Fish Commission under annual scientific collecting permits. Also, I am grateful to the many graduate students at Arkansas State University for their field assistance.

Literature Cited

Austin CR and **CL Baker.** 1964. Spermatozoon of *Pseudobranchus striatus axanthus*. Journal of Reproduction and Fertility 7:123–25.

Cope ED. 1889. The Batrachia of North America. Bulletin of the United States National Museum 34:1–575.

Dawes CJ. 1988. Introduction to biological electron microscopy: theory and techniques. Ladd Research Industries, Inc., Burlington (VT). 315 p.

Frost DR, T Grant, J Faivovich, RH Bain, A Haas, CFB Haddad, RO De Sá, A Channing, M Wilkinson, SC Donnellan, CJ Raxworthy, JA Campbell, BL Blotto, P Moler, RC Drewes, RA Nussbaum, JD Lynch, DM Green, and **WC Wheeler.** 2006. The amphibian tree of life. Bulletin of the American Museum of Natural History 297:1–370.

Goin CJ and **OB Goin.** 1962. Introduction to Herpetology. W. H. Freeman and Co. San Francisco (CA). 341 p.

Goin CJ, OB Goin, and **GR Zug.** 1978. Introduction to Herpetology, 3rd ed. W. H. Freeman and Co. San Francisco (CA). 378 p.

Hanlin HG and **RH Mount.** 1978. Reproduction and activity of the greater siren, *Siren lacertina* (Amphibia: Sirenidae), in Alabama. Journal of the Alabama Academy of Science 49:31–39.

Martof BS. 1973. *Siren intermedia*. Catalogue of American Amphibians and Reptiles 127.1-127.3.

Martof BS. 1974. *Siren*. Catalogue of American Amphibians and Reptiles 152.1-152.2.

Noble GK and **BC Marshall.** 1932. The validity of *Siren intermedia* Leconte, with observations on its life history. American Museum Novitates 532:1-17.

Ogielska M and **J Bartmańska.** 2009. Spermatogenesis and male reproductive system in Amphibia—Anura. *In*: Ogielska M, editor. Reproduction in amphibians. CRC Press (Boca Raton, FL). p 34-99.

Presnell JK and **MP Schreibman.** 1997. Humason's animal tissue techniques, 5th ed. Johns Hopkins University Press, Baltimore (MD). 572 p.

Pyron RA and **JJ Wiens.** 2011. A large-scale phylogeny of Amphibia including over 2800 species, and a revised classification of extant frogs, salamanders, and caecilians. Molecular Phylogenetics and Evolution 61:543-83.

Ross MH, EJ Reith, and **LJ Romrell.** 1989. Histology: a text and atlas. Williams and Wilkins, Baltimore (MD). 783 p.

Sawyer JA and **SE Trauth.** 2012. Seasonal activity, population characteristics, and age estimation in the aquatic salamander, *Siren intermedia nettingi* (Goin). Journal of the Arkansas Academy of Science 64: 65:117-25.

Scheltinga DM and **BGM Jamieson.** 2003. The mature spermatozoon. *In:* Reproductive biology and phylogeny of Urodela. Sever DM editor, Science Publishers, Inc., Enfield (NH). p 203-74.

Sever DM. 1991. Comparative anatomy and phylogeny of the cloacae of salamanders (Amphibia: Caudata). II. Cryptobranchidae, Hynobiidae, and Sirenidae. Journal of Morphology 207:283-301.

Sever DM, LC Rania, and **JD Krenz.** 1996. Reproduction of the salamander *Siren intermedia* Le Conte with especial reference to oviducal anatomy and mode of fertilization. Journal of Morphology 227:335-48.

Trauth SE. 2020. Distal urogenital anatomy of male Prairie Racerunners, *Aspidoscelis sexlineatus viridis* (Reptilia: Sauria: Teiidae). Journal of the Arkansas Academy of Science 74:11-20.

Trauth SE. 2021. Morphology of Rathke's glands in the alligator snapping turtle, *Macrochelys temminckii* (Chelonia: Chelydridae). Journal of the Arkansas Academy of Science 75:45-51.

Trauth SE, HW Robison, and **MV Plummer.** 2004. The amphibians and reptiles of Arkansas. University of Arkansas Press, Fayetteville (AR). 421 p.

Trauth SE, DS Siegel, JS Godley, ZC Adcock, and **RW McDiarmid.** 2017. Testicular histology reveals a novel type of spermatogenesis in *Pseudobranchus axanthus* (Caudata: Sirenidae). Copeia 105:670-77.

Uribe MCA. 2003. The testes, spermatogenesis and male reproductive ducts, *In:* Reproductive biology and phylogeny of Urodela. Sever DM editor, Science Publishers, Inc., Enfield (NH). p 183-202.

Uribe MCA and **V Mejía-Roa.** 2014. Testicular structure and germ cells morphology in salamanders. Spermatogenesis 4:1-12. DOI: http://dx.doi.org/10.4161/21565562.2014.988090.

Uribe MCA, HJ Grier, and **V Mejía-Roa.** 2014. Comparative testicular structure and spermatogenesis in bony fishes. Spermatogenesis 4:1-13. DOI: http://dx.doi.org/10.4161/21565562.2014.983400.

Uribe MCA, G Gómez Rios, and **RA Brandon.** 1994. Spermatogenesis in the urodele *Ambystoma dumerlii*. Journal of Morphology 222:287-99.

Willett JA. 1965. The male urogenital system in the Sirenidae. Journal of the Tennessee Academy of Science 40:9-17.

Yoshida S. 2016. From cyst to tubule: innovations in vertebrate spermatogenesis. WIREs Developmental Biology 5:119-31.

Zhang P and **DB Wake.** 2009. Higher-level salamander relationships and divergence dates inferred from complete mitochondrial genomes. Molecular Phylogenetics and Evolution 53:492-508.

Specimens Examined – (ASUMZ nos. in monthly order): ASUMZ 30336, —, 11 Jan 2007; ASUMZ 30337, —, 11 Jan 2007; ASUMZ 31582, 221, 18 Jan 2011; ASUMZ 32416, 273, 21 Jan 2013; ASUMZ 30345, —, 26 Jan 2007; ASUMZ 22274, 234, 22 Feb 1998; ASUMZ 31985, 236, 24 Feb 2012; ASUMZ 19342, —, 28 Feb 1994; ASUMZ 30416, —, 4 Mar 2007; ASUMZ 31620, 208, 15 Mar 2011; ASUMZ 21503, 236, 18 Mar 1997; ASUMZ 32586, 237, 19 Mar 2013; ASUMZ 32588, 228, 19 Mar 2013; ASUMZ 33189, 266, 4 May 2014; ASUMZ 33201, 277, 23 May 2014; ASUMZ 33239, 270, 19 Jun 2014; ASUMZ 32309, 283, 16 Jul 2012; ASUMZ 32311, 270, 16 Jul 2012; ASUMZ 33370, 278, 19 Aug 2015; ASUMZ 32366, 242, 11 Oct 2012; ASUMZ 33318, 278, 31 Oct 2014; ASUMZ 33329, 218, 7 Dec 2014.

https://scholarworks.uark.edu/jaas/vol76/iss1/5

DOI: 10.54119/jaas.2022.7604